Markov Models of DC Microgrid Architectures

Francesco Di Gregorio, Gilles Sassatelli, Abdoulaye Gamatié

Markov Models of DC Microgrid Architectures

Francesco Di Gregorio, Gilles Sassatelli, Abdoulaye Gamatié

I. Introduction

The Markov models [1] of the ring, ladder, and crossbar-based DC microgrid architectures are extracted in this annex. Since the ladder and crossbar-based architectures have two diverse types of source-load connections, they are modeled by two different Markov models. Then, in total, there are five Markov models corresponding to the five use cases represented in Figure 2 that are named as follows: ring, ladder1, ladder2, crossbar1, crossbar2.

A. Markov model of a connection source-load.

Figure 1 shows the schematic of a simple connection source-load enabled by the switch $SW1$. Moreover, the Markov chain representing this connection is depicted.

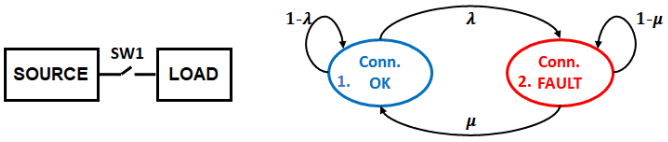

Fig. 1. Source-load connection Markov model.

Here, states 1 and 2 denote the state of the switch SW1. When we are in state 1, the switch is working, and the connection can be established. On the other hand, when we are in state 2, the switch is in a failure condition, and then it cannot be employed to create this connection. The arrows represent the transition probabilities. For instance, the probability to transit from state 1 to state 2 is given by $\lambda \Delta t$ where λ is the failure rate of the switch SW1, and Δt represents the considered interval of time. Subsequently, if the model is evaluated each hour, the failure rate in [failures/hours] directly gives the transition probability.

Moreover, another property of a Markov model is the sum of steady-state probabilities of each state has to be equal to the unity, as follows:

$$\sum_{i=1}^{N} P_{Si} = 1 \tag{1}$$

where P_{Si} represents the steady-state probability of being in state i and N is the number of states of the Markov model. This equation is referred in literature to as the normalization equation. From this diagram, the following equation in matrix form can be derived.

$$\begin{bmatrix} -\lambda & \mu \\ \lambda & -\mu \end{bmatrix} X \begin{bmatrix} P_{S1} \\ P_{S2} \end{bmatrix} = \begin{bmatrix} 0 \\ 0 \end{bmatrix} \tag{2}$$

where P_{S1} represents the steady-state probability of being in state 1 and P_{S2} is the steady-state probability of being in state 2. From (2), and using the normalization equation in (1), one can calculate the steady-state probabilities of each state. If we divide the set of states into S safe states and F faulty states, we obtain the availability and unavailability of the system as:

$$U = \sum_{i=1}^{F} P_{FSi}, \quad A = \sum_{n=1}^{S} P_{SSn} \tag{3}$$

where P_{FSi} represents the steady-state probability of the faulty state i and P_{SSi} is the steady-state probability of the safe state n.

II. Markov model of DCMG Architectures

This section describes the calculation of the reliability of a DCMG architecture when considering the repair of components. The obtained model is more faithful to reality because it considers a fault on a switch can be detected and replaced within a specific time interval. Markov chains are used as a mathematical tool to model the DCMG architecture and determine the MTBF of the system. The model considers all the cases which lead to a connection fault.

A connection fault represents a condition where a source cannot supply a load because all available paths are faulty. The repair rate μ is defined as the rate at which faulty components are replaced.

States of the Markov models, in our application, represent different fault stages of the system. In fact, starting from the state where all components are OK, the system could transit in states where some fault on non-critical components let the system continue working. Ultimately, chains terminate when a state representing a critical system fault is reached. In these states, the system is considered down, and only a repair operation could let the system works again.

Then, by solving the Markov model, it is possible to determine the steady-state probability of faulting a connection source-load related to the connection's availability. Finally, by using equations (3), the availability of the architecture can be retrieved.

A. Ring Architecture

Figure 2 a) shows the ring architecture highlighting an example of connection source-load between Battery 2 (B2) and DC Load 2 (DL2).

In this case, the principal causes that bring a connection failure are two. The first is a fault in one of the terminal switches. The second consists in having a consecutive fault on both the semi-arcs of the ring. For instance, the connection Battery 2 (B2) $\rightarrow$ DC Load 2 presents $2 * n_1$ switches on the shortest semi-arc of the ring and $2 * n_2$ switches on the longest semi-arc of the ring, as shown in Figure 2 a).

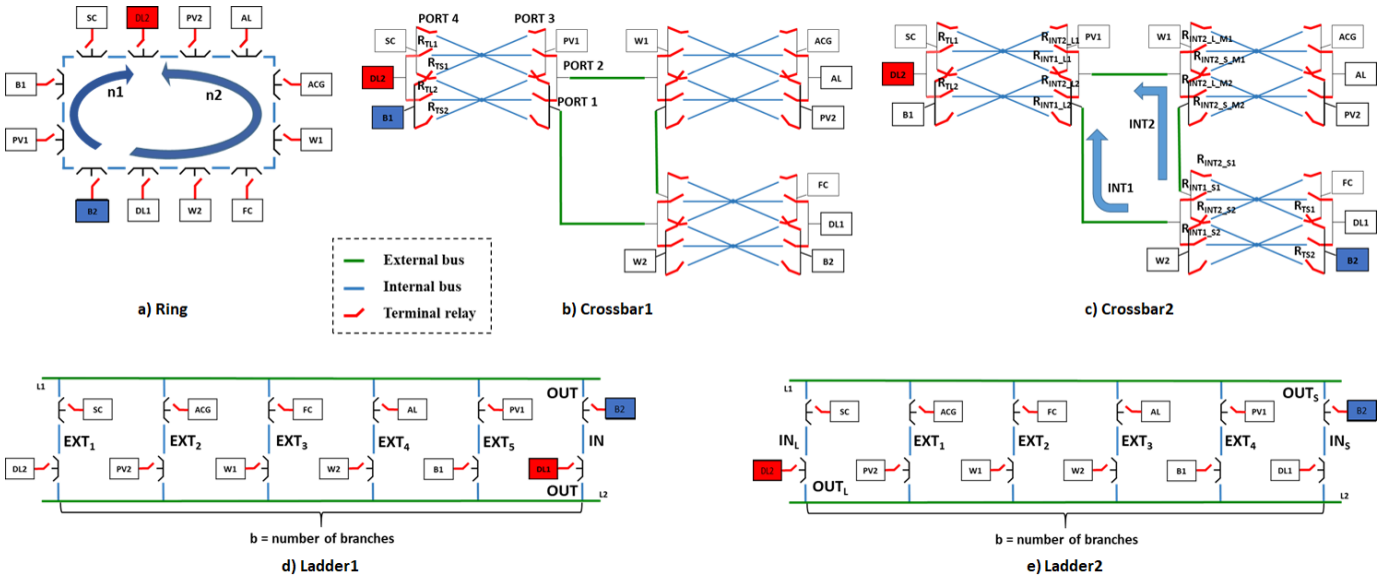

Fig. 2. DCMG benchmark extracted from [2]: a) Ring, b) Ladder case 1, c) Ladder case 2, d) Crossbar case 1, e) Crossbar case 2.

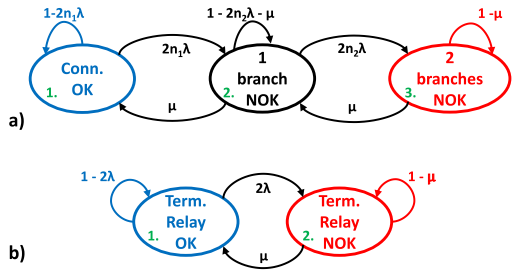

Fig. 3. Markov model of the ring architecture: a) Ring and b) Terminal sub-module.

Since we assume the hypothesis of independent components, the two principal causes of fault are independent as well. Therefore, a modular approach can be adopted as explained in [3].

From the foregoing considerations, two sub-modules are found in the ring architecture that corresponds to the two leading causes of connection fault explained above, as shown in Figure 3 a) and b). Moreover, the series connection of n switches is modeled as a single state having a failure rate $n\lambda$ [4].

Figure 3 a) represents the Markov model of the two semi-arcs of the ring, where the state S2 corresponds to a fault on one of the $2 * n_1$ switches of the first branch and the state S3 corresponds to a consecutive fault of both branches. Finally, the transition probability for these states is $2 * n_1 * \lambda$ and $2 * n_2 * \lambda$, respectively.

Figure 3 b) represents the Markov model of the terminal switches, retrieved with the same method.

Once the two Markov models are solved, the availability and unavailability of the two sub-modules are retrieved. Therefore, the probability of having a critical connection fault is determined by the following algebraic formula:

$$A_{Ring} = A_{sub1} * A_{sub2} \tag{4}$$

where U_{ring} is the overall unavailability of the connection Battery 2 $\rightarrow$ DC Load 2, A_{sub1} and A_{sub2} represent the availability of the two sub-modules in Figure 3 a) and b).

B. Ladder Architecture: Use case 1

Figure 2 d) shows a schematic of the ladder architecture in the first use case. We can distinguish three types of switches: terminal switches that permit the connection of the EP to the DCMG, and IN/OUT switches that allow connection to the internal part of the branch or the external bus, respectively. Then, three principal causes of a connection failure are identified:

1) a fault on a terminal switch;
2) a fault on a IN switch && OUT switch of source or load;
3) a fault on a IN switch && all the external branches (EXTx).

Based on these assumptions, two independent sub-modules are identified. The first relates to the terminal switches. The corresponding Markov model is depicted in Figure 4 c). The second relates to the other two fault causes. The corresponding sub-module is depicted in Figure 4 b). Since the external branches are independent with respect to the IN and OUT switches, they can be handled separately in a sub-sub-module as depicted in Figure 4 d).

Subsequently, the resolution of this model is executed hierarchically. First, the sub-sub-module representing the external branches is solved. Availability and unavailability of the latter are retrieved and used to obtain the equivalent failure rate λ_{eq}, as shown in Figure 4 b). Then, the Markov models of the two sub-modules are solved separately.

Ultimately, the availability of the ladder architecture is obtained as follows:

$$A_{ladder1} = A_{sub1} * A_{sub2} \tag{5}$$

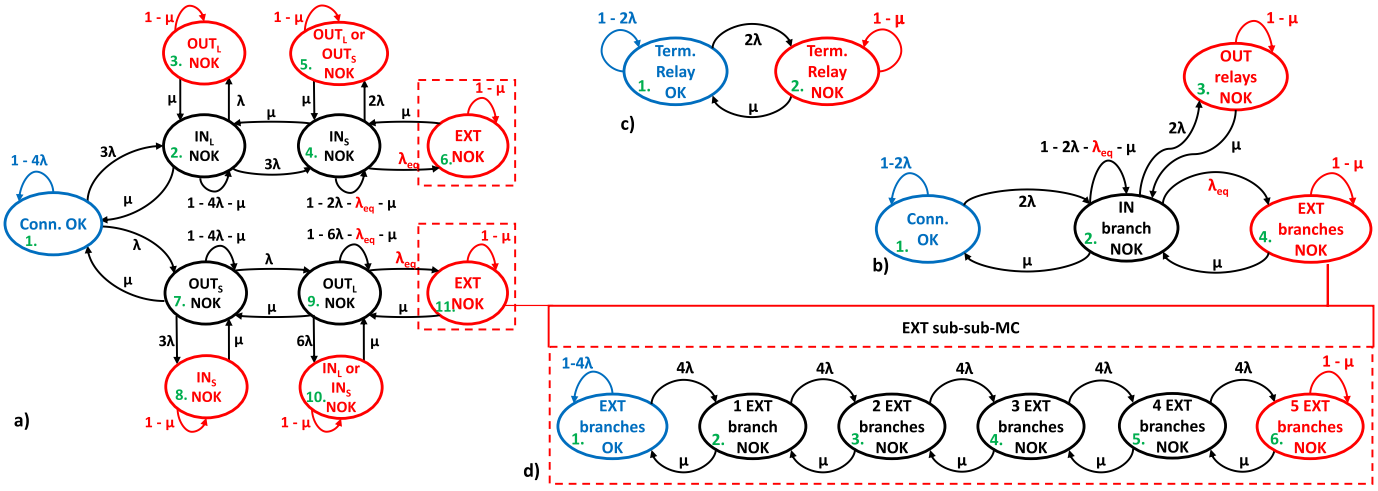

Fig. 4. Markov model of the Ladder architecture in the two use cases: a) Ladder2 main sub-MC, b) Ladder1 main sub-MC, c) terminal switches MC and d) external branches MC.

where A_{sub1} represents the availability obtained solving the Markov model in Figure 4 c) and the A_{sub2} is the availability obtained solving the Markov model in Figure 4 b).

III. Ladder Architecture: Use Case 2

Figure 2 e) shows an example of the connection of a ladder architecture in the second case where source and load belong to different steps of the ladder.

In particular, in this case, a connection fault occurs in the following conditions:

1) a fault on a terminal switch of source or load;
2) a fault on both IN and OUT switches of the source or the load
3) a fault on IN-IN or OUT-OUT relays together with all the external branches (EXTx)

Based on these assumptions, two independent sub-modules are identified in the DFT of this connection. The first relates to the terminal switches. The corresponding Markov model is depicted in Figure 4 c). The second relates to the other two fault causes. The corresponding sub-module is depicted in Figure 4 a). Since the external branches are independent of the IN and OUT switches, they can be considered separately in a sub-sub-module as depicted in Figure 4 d).

Then, the model is solved recursively. Initially, the sub-sub-MC related to the External branches is solved, and an equivalent failure rate λ_{eq} is calculated. Then, the sub-MC in Figure 4 a) is solved by using the retrieved λ_{eq} and the unavailability U_{sub2} of the sub-MC is obtained.

On the other hand, the terminal relay MC in Figure 4 c) is solved independently retrieving its availability A_{sub1}.

$$A_{ladder2} = A_{sub1} * A_{sub2} \tag{6}$$

A. Crossbar-based Architecture: Use Case 1

The connection between Battery 1 (B1) and DC Load 2 (DL2) is considered for the first case, as shown in Figure 2 b).

In the crossbar-based architecture, we can distinguish two types of switches: terminal switches that permit the connection between an EP and the DCMG and interconnection switches that are used to connect the crossbars. On the other hand, Internal busses are used for the energy sharing between EPs connected to the same crossbar, and External busses are used to create inter-crossbar connections.

Therefore, a connection fault occurs in the following conditions:

1) A fault on all terminal switches of a source or load. Notice that the crossbar-based architecture has more than one terminal switch per EP. This improves the reliability of the connection because of the redundancy of the most critical component.
2) if each bus presents at least a terminal relay in fault && all the other crossbar ports present at least a fault each.

Based on these assumptions, the Markov model of the crossbar-based architecture is retrieved as shown in Figure 5 a). As for the ladder architecture, the crossbar also presents an independent sub-MC representing the state of the other ports of the crossbar, as shown in Figure 5 d). In this work, other ports refer to the ports of the crossbar not directly involved in the source-load connection.

Then, the obtained Markov model is solved hierarchically. Initially, the sub-MC related to the other ports of the crossbar is solved, and its equivalent failure rate λ_{eq} is retrieved. Second, by using the λ_{eq}, the overall MC in Figure 5 a) is solved and the availability $A_{crossbar1}$ of the connection is retrieved.

B. Crossbar-based Architecture: Use Case 2

Figure 2 c) shows a schematic of the second connection case. Here, the Markov model depends on how the crossbars are interconnected. A connection fault occurs in the following conditions:

1) a fault on a terminal port (both terminal switches of a source or load);

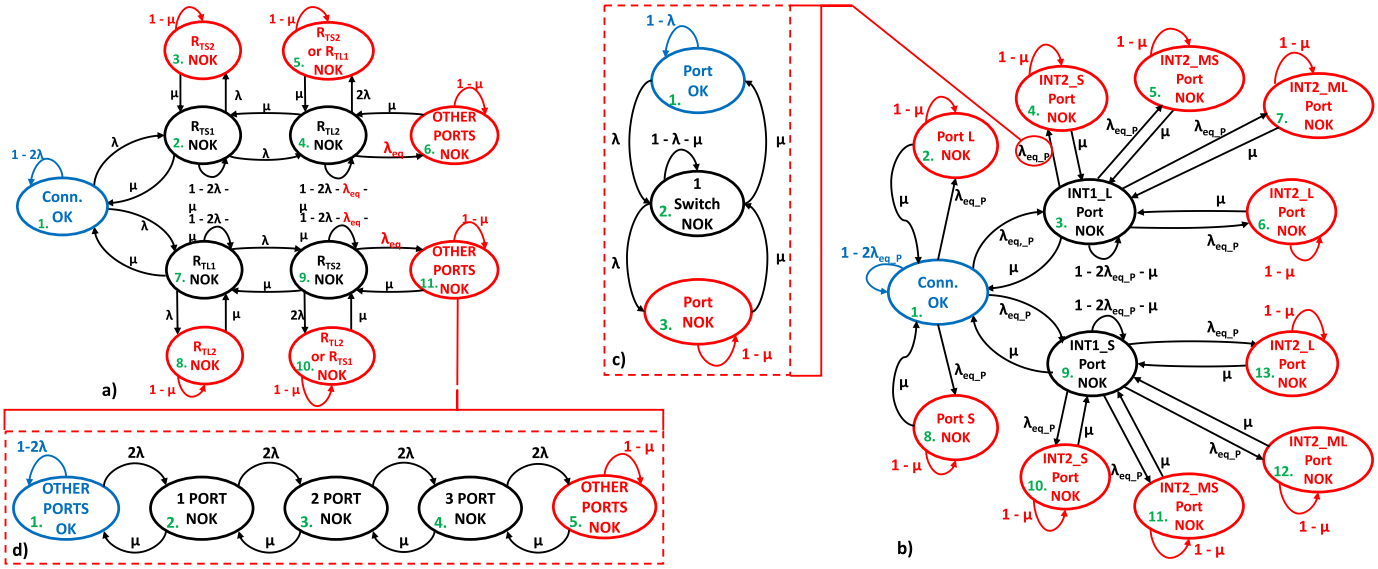

Fig. 5. Markov model of the Crossbar-based DCMG architecture: source and load are connected to the same crossbar.

2) interconnection ports of the crossbars of the source and load are faulty;
3) interconnection ports of intermediate crossbars (if any) allowing the crossbars of the source and load to connect are at fault.

The first cause is the most critical because it involves specific ports (the ones that connect the source and load to the DCMG). The second cause depends on the relationship between the interconnection ports of the crossbars connected to the source and load. We can say that two interconnection ports belonging to different crossbars are related if at least a path in the DCMG permits their connection. Once the relationships between interconnection ports are found, the transition probabilities can be calculated.

The third cause is related to the specific implementation. In fact, it depends on the reliability of all redundant paths through the crossbar network that allows the connection between the considered source and load. Then, considering the reliability of each path, we can obtain the probability of a connection failure. Since the crossbar-based architecture presents high flexibility, many redundant paths can be found even in small implementations. Therefore, the probability of having consecutive faults in all redundant paths becomes extremely low and therefore negligible.

For this reason, we can approximate the Markov model of the crossbar-based DCMG in the second case considering just the first two connection fault causes. Moreover, this approximation has the advantage of making the model independent from the specific implementation. Note that the larger the microgrid size, the more this approximation is valid because of the increase in path redundancy. Figure 5 b) shows the Markov model of the crossbar-based DCMG for the second connection type. Furthermore, in order to determine the failure rate of a port, the sub-MC in Figure 5 c) is used.

REFERENCES

[1] X. Jia, J. Shen, and R. Xing, "Reliability analysis for repairable multistate two-unit series systems when repair time can be neglected," *IEEE Transactions on Reliability*, vol. 65, no. 1, pp. 208–216, 2016.
[2] F. Di Gregorio, G. Sassatelli, A. Gamatié, and A. Castelltort, "A flexible power crossbar-based architecture for software-defined power domains," in *2020 22nd European Conference on Power Electronics and Applications (EPE'20 ECCE Europe)*, 2020, pp. 1–9.
[3] S. Kabir, K. Aslansefat, I. Sorokos, Y. Papadopoulos, and S. Konur, "A hybrid modular approach for dynamic fault tree analysis," *IEEE Access*, vol. 8, pp. 97 175–97 188, 2020.
[4] F. Di Gregorio, "Exploration of Dynamic Reconfiguration Solutions for Improved Reliability in DC Microgrids," Theses, Université de montpellier 2, Nov. 2021. [Online]. Available: https://hal.archives-ouvertes.fr/tel-03558951